Cell Reports

Article

The bacteriophage LUZ24 "Igy" peptide inhibits the *Pseudomonas* DNA gyrase

Graphical abstract

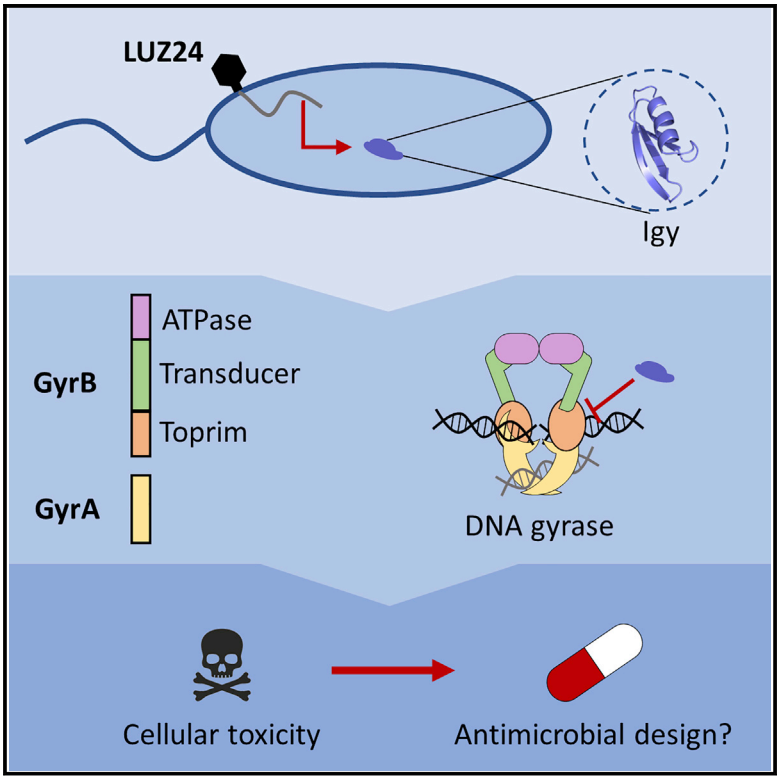

Authors

Jeroen De Smet, Jeroen Wagemans, Maarten Boon, ..., Dmitry Ghilarov, Konstantin Severinov, Rob Lavigne

Correspondence

rob.lavigne@kuleuven.be

In brief

De Smet et al. explore one of the orphan early genes of a bacteriophage infecting *Pseudomonas aeruginosa*. They reveal its activity as a gyrase inhibitor, with potential for drug development. As such, they offer an additional example of how this viral dark matter could be mined for biotechnological applications.

Highlights

- An early gene of phage LUZ24 inhibits the DNA gyrase subunit B of *P. aeruginosa*
- This gene is therefore coined Igy, inhibitor of gyrase
- Igy most likely interferes with the gyrase's ability to bind DNA by using DNA mimicry
- Igy holds potential for the development of antibiotics

De Smet et al., 2021, Cell Reports *36*, 109567
August 24, 2021
https://doi.org/10.1016/j.celrep.2021.109567

CellPress

Cell Reports

CellPress
OPEN ACCESS

Article

The bacteriophage LUZ24 "Igy" peptide inhibits the *Pseudomonas* DNA gyrase

Jeroen De Smet,[1,5] Jeroen Wagemans,[1] Maarten Boon,[1] Pieter-Jan Ceyssens,[1,6] Marleen Voet,[1] Jean-Paul Noben,[2] Julia Andreeva,[3] Dmitry Ghilarov,[3,7] Konstantin Severinov,[3,4] and Rob Lavigne[1,8,*]

[1]Laboratory of Gene Technology, Department of Biosystems, KU Leuven, 3001 Leuven, Belgium
[2]Biomedical Research Institute and Transnational University Limburg, School of Life Sciences, Hasselt University, 3590 Diepenbeek, Belgium
[3]Centre for Life Sciences, Skolkovo Institute of Science and Technology, 143026 Moscow, Russia
[4]Waksman Institute for Microbiology, Rutgers, The State University of New Jersey, Piscataway, NJ 08854, USA
[5]Present address: Research group for insect production and processing, Department of Microbial and Molecular Systems, KU Leuven, 2240 Geel, Belgium
[6]Present address: Division of Bacterial Diseases, Sciensano, 1050 Brussels, Belgium
[7]Present address: Malopolska Centre of Biotechnology, Jagiellonian University, 30387 Krakow, Poland
[8]Lead contact
*Correspondence: rob.lavigne@kuleuven.be
https://doi.org/10.1016/j.celrep.2021.109567

SUMMARY

The bacterial DNA gyrase complex (GyrA/GyrB) plays a crucial role during DNA replication and serves as a target for multiple antibiotics, including the fluoroquinolones. Despite it being a valuable antibiotics target, resistance emergence by pathogens including *Pseudomonas aeruginosa* are proving problematic. Here, we describe Igy, a peptide inhibitor of gyrase, encoded by *Pseudomonas* bacteriophage LUZ24 and other members of the *Bruynoghevirus* genus. Igy (5.6 kDa) inhibits *in vitro* gyrase activity and interacts with the *P. aeruginosa* GyrB subunit, possibly by DNA mimicry, as indicated by a *de novo* model of the peptide and mutagenesis. *In vivo*, overproduction of Igy blocks DNA replication and leads to cell death also in fluoroquinolone-resistant bacterial isolates. These data highlight the potential of discovering phage-inspired leads for antibiotics development, supported by co-evolution, as Igy may serve as a scaffold for small molecule mimicry to target the DNA gyrase complex, without cross-resistance to existing molecules.

INTRODUCTION

The pathogenic bacterium *Pseudomonas aeruginosa* is known for its extreme metabolic versatility and complex regulatory potential (Stover et al., 2000). For this bacterium, antibiotic resistance is often driven by mutations within the components of its multiprotein complexes. A representative example here is the DNA gyrase complex, which plays an important role in reducing the torsional stress in the DNA during processes such as DNA replication by introducing negative supercoils (Collin et al., 2011). To introduce negative supercoils, one of the double-stranded DNA (dsDNA) strands is cleaved and immobilized to allow the passage of the other dsDNA strand (Collin et al., 2011).

The gyrase complex consists of a heterotetramer of two GyrB and two GyrA subunits (Higgins et al., 1978). GyrA contains four domains, namely, a winged-helix domain (WHD), a tower domain, a coiled-coil domain, and the C-terminal domain. The WHDs and the globular domains, formed by the ends of the coiled-coil domains, stabilize dimerization of the GyrA subunits (Morais Cabral et al., 1997; Weidlich and Klostermeier, 2020). This results in the formation of two interfaces, namely, the DNA-gate and the C-gate for the WHDs and the globular domains, respectively (Morais Cabral et al., 1997; Weidlich and Klostermeier, 2020). GyrB consists of the following three domains: an ATPase domain of the GHKL (GyrB-Hsp90-histidine/serine protein kinases-MutL) superfamily, a transducer domain, and a topoisomerase-primase (TOPRIM) domain (Weidlich and Klostermeier, 2020; Wigley et al., 1991). Upon the binding of ATP, GyrB dimerizes to form the third interface, the N-gate (Hartmann et al., 2017; Wigley et al., 1991). Interactions between the GyrB TOPRIM domain and the WHDs of GyrA aid in the formation of the DNA-gate (Morais Cabral et al., 1997; Schoeffler et al., 2010).

Some organism- or group-specific differences in the structure of both gyrase subunits that could modulate the interactions and the function of the complex have been observed. One example is insertions in the GyrB TOPRIM domain in several Gram-negative bacteria that are absent in homologs from Gram-positive bacteria (Schoeffler et al., 2010). In the *Escherichia coli* GyrB, such ~170-amino acid inserts form a globular domain with an α/β fold, contacts the coiled-coil domain of GyrA, and appears to play a role in DNA binding and interdomain communication of the enzyme (Schoeffler et al., 2010).

Because the DNA gyrase complex is essential in bacteria and is absent in mammalian cells, it is one of the most investigated and best validated targets for antibacterial agents with selective

toxicity. Many natural and synthetic inhibitors that either inhibit the catalytic activity of the gyrase complex (e.g., aminocoumarins) or block the process after the DNA cleavage (Tomašić and Mašič, 2014) (e.g., fluoroquinolones [Fàbrega et al., 2009]) are already known (Khan et al., 2018). However, a number of resistant isolates have already been reported for many of the inhibitors in several bacterial species, including *P. aeruginosa*. Two main resistance mechanisms to fluoroquinolones emerge in *P. aeruginosa* (Bruchmann et al., 2013), as follows: overexpression of resistance-nodulation-division efflux pumps, like MexXY-OprM, and spontaneous mutations in the quinolone-resistance-determining regions (QRDRs) of GyrA and GyrB. Transferable resistance mechanisms, determined by *qnr* genes encoding gyrase-binding DNA-mimic proteins, are also coming into focus (Ruiz, 2019).

Bacteriophages have evolved unique proteins that interact with essential components of their bacterial hosts that redirect host physiology to serve the needs of the virus (De Smet et al., 2017). To date, many phage-encoded genes remain as ORFans with no sequence similarity to known genes and no functional predictions (Yin and Fischer, 2008). By identifying and mimicking phage proteins that interact with host proteins and alter crucial host functions, this viral dark matter could be harnessed as a source of novel antimicrobials (Projan, 2004). Liu et al. (2004) showed the feasibility of such an approach by identifying compounds that mimicked toxic phage-host interactions and were active against *Staphylococcus aureus* (Liu et al., 2004).

Within this context, it was our aim to explore the many *Pseudomonas* phage genes, which encode early phage proteins that could potentially inhibit *P. aeruginosa* growth (Van den Bossche et al., 2014; Wagemans et al., 2014). Indeed, a previous study mining the LUZ24 phage proteome for antibacterial proteins resulted in the identification of four inhibitory phage proteins (Wagemans et al., 2015). Expression of one of these proteins, namely, LUZ24 gp9, prevented colony formation and caused severe filamentous growth in *P. aeruginosa* strains PAO1 and PA14. We show here that LUZ24 gp9 (Igy) is an inhibitor of the DNA gyrase. It interacts with GyrB and blocks bacterial DNA replication. Because Igy has no cross-resistance to fluoroquinolones, it has an excellent potential as a phage-inspired lead for antibiotics development and for other biotechnological applications.

RESULTS AND DISCUSSION

The DNA gyrase B subunit is the target of LUZ24 gp9

LUZ24 gp9 is a small (5.6 kDa and 48 amino acids [aa]) polypeptide with close homologs found in six other related *Pseudomonas* phages (MR299-2, vB_PaeP_C1-14_Or, PaP3, PaP4, phiIBB-PAA2, and TL), belonging to the *Bruynoghevirus* genus. Aside from its conservation among most members of this genus, no sequence similarity (e-value, $<1.10^{-5}$) can be found to any known protein, suggesting a specific biological role within this clade of viruses. We previously showed that expression of LUZ24 gp9 resulted in severe filamentous growth in *P. aeruginosa* strains PAO1 and PA14 but did not affect the growth of *E. coli* MG1655 (Wagemans et al., 2015). With a mass of only 5.6 kDa and no predicted catalytic domains, gp9 most likely exerts its effect on host physiology through a protein-protein interaction with an essential target.

Because a prior interaction assay remained inconclusive (Wagemans et al., 2015), an *in vitro* pull-down assay using recombinant glutathione S-transferase (GST)-tagged gp9 was performed to identify the interaction partner in *P. aeruginosa* cell extracts. To avoid sterical hindrance of the affinity tag during the pull-down assay, a linker sequence separated the GST-tag from the gp9 sequence, making the phage peptide more exposed. Proteins recovered from the *P. aeruginosa* extract in the pull-down assay with the gp9 fusion as a bait were compared to a negative control of purified LUZ24 gp9-GST from the *E. coli* BL21 cell extract to exclude false-positive binding proteins. After the pull-down with *P. aeruginosa* PAO1 extract, two additional ~110-kDa bands were co-purified with gp9 as judged by SDS-PAGE (Figure 1A). Compared to the controls, mass spectrometric analysis identified peptides from four host proteins as potential interaction partners, as follows: the Lon protease, the DNA gyrase subunit B, the NADH dehydrogenase subunit G, and the bifunctional aconitrate hydratase 2/2-methylisocitrate dehydratase AcnB (Figure 1B; Table S1). Because these last two proteins co-purified non-specifically in pull-downs of other protein complexes (DnaX/AcpP and Hfq/MvaT/AcpP, respectively) as previously described (Van den Bossche et al., 2014), they were excluded from the interaction candidates list. Moreover, because the expression of gp9 in a *Δlon* mutant did not alter the toxicity of the phage protein, the Lon protease was also excluded as a direct bacterial target of gp9 (Figure S1), leaving the DNA gyrase subunit B as the most promising interaction candidate. This was further supported by the fact that phages are known to encode topoisomerase inhibitors, as was shown by the identification of a phage-encoded inhibitor of topoisomerase I function in the coliphage T4 (Mattenberger et al., 2015). Furthermore, expression of LUZ24 gp9 results in filamentous growth, which is consistent with the activation of the SOS response after inhibition of gyrase activity (Nakanishi et al., 1998).

To gain additional insights, a complementation assay using a random genome fragment library from *P. aeruginosa* PAO1 was performed to identify host proteins that could prevent gp9 toxicity. This assay identified a total of 13 clones, in which no toxicity of gp9 was observed. All recovered clones contained plasmids harboring a common region of the PAO1 genome with the PA4472/*tldE* and PA4474/*tldD* genes in the sense orientation (Table S2). The products of these genes form subunits of a metalloprotease that processes the precursors of microcin B17 and CcdA (Allali et al., 2002). Microcin B17 is a peptide antibiotic that targets the DNA gyrase in *E. coli* (Collin and Maxwell, 2019), whereas CcdA is the antitoxin for the toxin CcdB that targets the GyrA subunit (Van Melderen et al., 1994). To test the hypothesis that gp9 might also be recognized as the TldD/E substrate, recombinant TldD and TldE were combined with gp9 *in vitro*. A MALDI-TOF analysis confirmed that gp9 was indeed degraded by TldD/E to fragments of 1–2 kDa (Figure S2). Plasmids expressing resulting fragments of gp9 were constructed, and they were found to be no longer toxic at conditions of induction (Figure S3). We therefore conclude that TldD/E likely prevents the toxicity of gp9 by degrading the peptide.

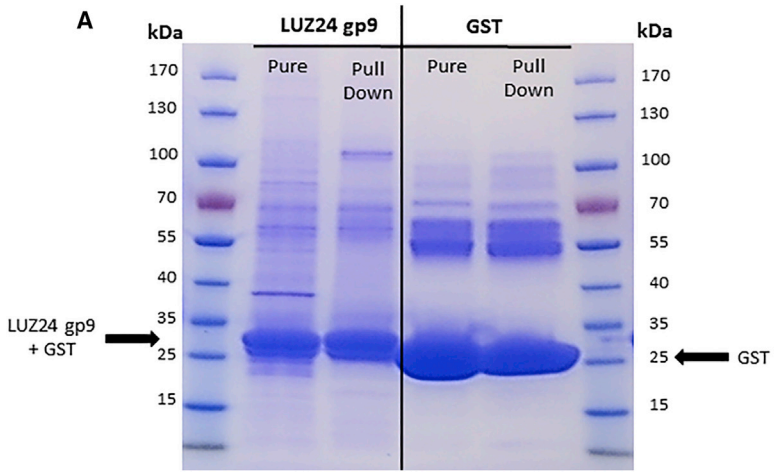

B

Protein	kDa	#
Lon protease	89	107
NADH dehydrogenase subunit G	99	28
DNA gyrase subunit B	90	11
Bifunctional aconitrate hydratase 2 /2-methylisocitrate dehydratase	94	4

Figure 1. Pull-down reveals four proteins as potential interaction partners for LUZ24 gp9

(A) SDS-PAGE gel with the *in vitro* pull-down samples. From left to right: PageRuler ladder, LUZ24 gp9-GST fusion (32.4 kDa) after affinity purification, LUZ24 gp9-GST associated material from the PAO1 lysate, GST (27 kDa) after affinity purification, and GST-associated material from the PAO1 lysate.

(B) List of the mass spectrometry results for proteins uniquely identified in the ~100-kDa range in the LUZ24 gp9 pull-down sample, with their mass and the number of identified peptides. See also Table S1.

Next, to confirm the interaction between gp9 and the DNA gyrase subunit, bacterial two-hybrid (B2H) constructs containing the complete DNA gyrase B subunit and five overlapping GyrB fragments were prepared and tested with a gp9 B2H construct as a bait (Figure 2A). For one GyrB fragment construct, GyrB_2, a significant ($p < 0.01$, compared to the empty vector controls) increased production of β-galactosidase (approx. 1,188 Miller units) was observed (Figure 2B). No interactions with the full protein could be found, which might be due to sterical hindrance of the T25 or T18 fragment that prevents gp9 from binding its target.

The DNA gyrase B subunit interaction region defined in B2H assay includes both the part of the transducer domain with the ATP binding site and the dimerization interface. Binding of gp9 at either of these locations could interfere with normal gyrase functioning.

Gp9 or Igy inhibits the enzymatic activity of *P. aeruginosa* DNA gyrase

To determine whether the interaction of gp9 with the PAO1 gyrase is responsible for the earlier observed *in vivo* toxicity, we monitored the growth of *E. coli* cells transformed with plasmids overproducing gp9 (pHERD20T_gp9) and *P. aeruginosa* PAO1 or *E. coli* gyrase subunits (pColA_gyrAB). Overexpression of gp9 alone or *E. coli* and PAO1 gyrase alone was not toxic. In contrast, co-overexpression of gp9 and PAO1 (but interestingly not *E. coli*) gyrase led to a ~100-fold decrease of colony-forming unit (CFU) number after 3 h of induction (Figure 3).

Next, to test the effect of the interaction between LUZ24 gp9 and the PAO1 DNA gyrase on its activity, an *in vitro* gyrase activity assay was performed. First, the effect of gp9 on the supercoiling activity of PAO1 gyrase was investigated and compared to the effect of the fluoroquinolone ciprofloxacin (CFX). As can be seen from Figure 4A, purified gp9 inhibited the gyrase activity at concentrations of 12.5 μM. The removal of the N-terminal-fused maltose binding protein (MBP)-tag was essential for this inhibition to occur, which is consistent with observations made during the full-length B2H analysis. Therefore, we renamed LUZ24 gp9 to Igy (inhibitor of gyrase). Known gyrase inhibitors belong to the following three main groups: with some preventing the ATPase activity; others inhibiting DNA binding; and some acting as "gyrase poisons" i.e., by stabilizing the temporary covalent complex between the enzyme and DNA, thereby leading to the formation of double-stranded breaks. CFX is an example of such a "gyrase poison." To further investigate the Igy mode of action, we carried out a gyrase cleavage assay for which the ability of an inhibitor to be a gyrase poison by stabilizing cleavage complex formation is monitored. The results of the cleavage assay shown in Figure 4B demonstrate that in contrast to CFX, gp9 decreases the formation of the DNA gyrase-DNA cleavage complex, implying that it might interfere with DNA binding similarly to characterized inhibitors such as simocyclinone D8 or QnrB/MfpA (Feng et al., 2021; Flatman et al., 2005a; Hegde et al., 2011; Mazurek et al., 2021).

The inhibition mechanism of Igy differs from the mode of action of fluoroquinolones

The binding of Igy to the DNA gyrase GyrB subunit and the results of the *in vitro* gyrase activity assays hint at a distinct mode of action for Igy compared to that for CFX. To further explore this action, we set out to confirm the absence of cross-resistance between CFX and Igy *in vivo* by expressing Igy in four CFX-resistant *P. aeruginosa* strains, namely, BR776, 10BR1, LW1047, and C038791 (Pirnay et al., 2009). Figure 5 indicates that the inhibition of the gyrase by Igy clearly differs from that of fluoroquinolones because no cross-resistance can be observed.

A *de novo* model hints that gyrase inhibition might be established through DNA mimicry

In general, two main strategies are used by gyrase inhibitors, namely, they either prevent binding of the DNA to the gyrase

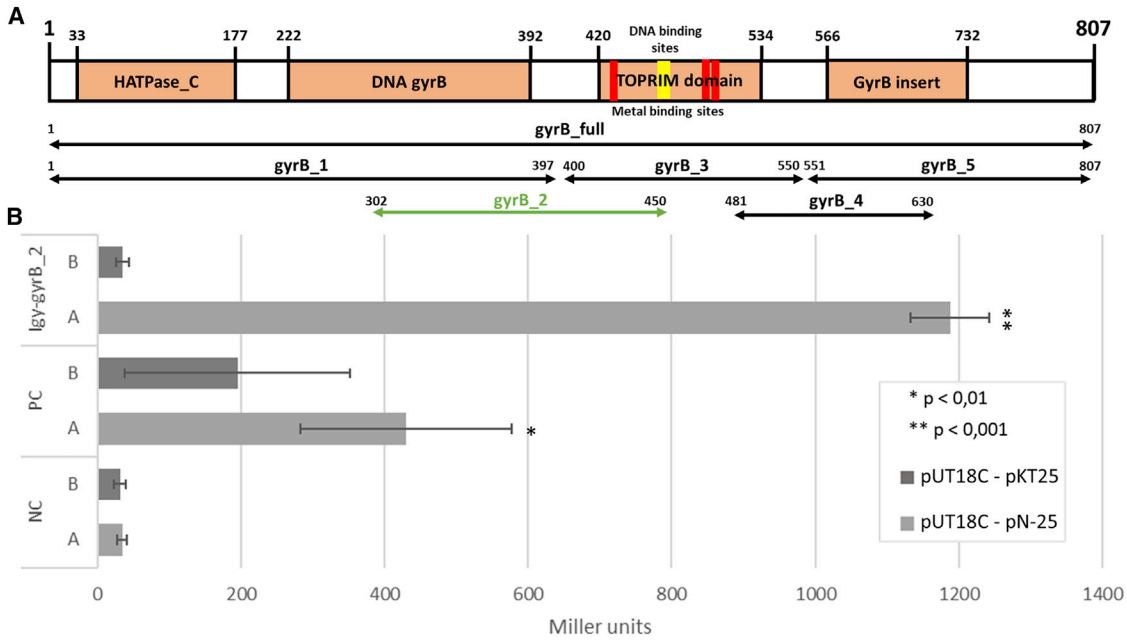

Figure 2. Bacterial two-hybrid assay of Igy with gyrase subunit B

(A) Schematic overview of the gyrase B subunit and the length of the selected fragments that were tested. Numbers indicate amino acids in protein, and the figure illustrates the significant positive hits.

(B) Overview of the Miller assay from the tested interactions for two plasmid combinations. As negative control (NC), empty plasmids were used and the dimerization of the ZIP protein was used as positive control. The β-galactosidase activity was measured quantitatively in Miller units. The assay was done in triplicate (n = 3). The error bars represent the standard deviation, and p values were calculated using Student's t test; *p < 0.01 and **p < 0.001.

(e.g., simocyclinone D8) or block the activity of gyrase to introduce breaks in the genome (e.g., fluoroquinolones) (Flatman et al., 2005a). To obtain mechanistic insights into what could be the inhibition mechanism of Igy, we modeled its structure *de novo* by using the QUARK algorithm (Xu and Zhang, 2012). The top scoring model showed a globular protein with a three-stranded β sheet and a protruding α-helix (Figure 6A; Data S1).

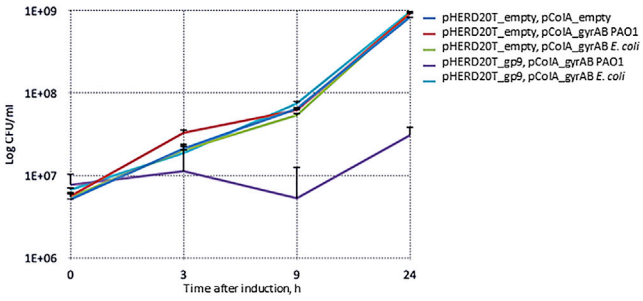

Figure 3. *In vivo* toxicity of LUZ24 gp9 in combination with *P. aeruginosa* or *E. coli* gyrase

The growth of *E. coli* cells transformed with pHERD20T plasmids overproducing gp9 and *P. aeruginosa* PAO1 or *E. coli* gyrase subunits was monitored. Overexpression of gp9 or *E. coli*/PAO1 gyrase alone was not toxic. In contrast, co-overexpression of gp9 and PAO1 gyrase led to a ~100-fold decrease of colony forming units (CFUs) at 3 h after induction. Three replicates were monitored per condition (n = 3). Error bars represent the standard deviation.

When comparing this structure to other known structures from the PDB database by using PDBeFold (Krissinel and Henrick, 2004), we retrieved multiple hits with phage proteins that inhibit DNA biosynthesis enzymes. Hits included (from highest to lowest score) the uracil-DNA glycosylase inhibitor P56 of *Bacillus* phage phi29 (PDB: 3ZOQ; Baños-Sanz et al., 2013), the RNA polymerase ε subunit of *Geobacillus stearothermophilus* (PDB: 4NJC; Keller et al., 2014), and the RNA polymerase inhibitor Gp2 of *E. coli* phage T7 (PDB: 4LK0; Bae et al., 2013). The best hit P56 is a small DNA mimicry protein that exhibits a negative charge distribution resembling that of the DNA phosphate-backbone (Figures 6B and 6C–6E). The negatively charged surface of P56 plays a key role in formation of the complex with the target (Baños-Sanz et al., 2013). Similar to P56, Igy also has a negative surface potential on the side of the helix (Figure 6D), suggesting Igy may function through a similar DNA mimicry mechanism to inhibit the gyrase. Interestingly, the C-terminal part of the determined interaction region (GyrB_2) encodes the edge of the presumed DNA-binding region of the TOPRIM region (Figure 2A). Other gyrase regulator proteins are known that prevent DNA binding to the gyrase such as YacG (Vos et al., 2014), GyrI (Chatterji and Nagaraja, 2002), and pentapeptide repeat proteins mentioned above; and it is known that GyrB plays a key part in binding of YacG, MfpA, and QnrB1.

Two mutations in the Igy sequence were recovered after screening *P. aeruginosa* colonies that formed after Igy expression from a plasmid, indicating a loss of toxicity of Igy. A change from glutamic acid in position 31 to lysine was found in 33

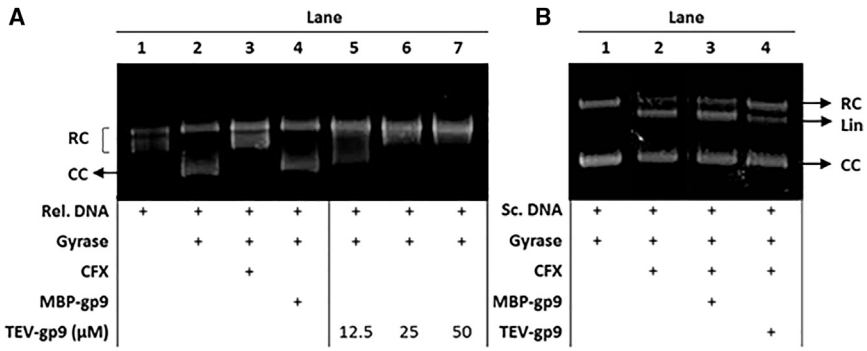

Figure 4. *In vitro* gyrase activity assays reveal inhibition of the gyrase activity by Igy

(A) *In vitro* supercoiling assay. On an agarose gel, the migration of relaxed DNA (lane 1) is affected when the DNA becomes supercoiled in the presence of gyrase (lane 2). This process in inhibited by ciprofloxacin (CFX; 30 μM; lane 3, positive control). Although the inhibition is not observed for MBP-Igy fusions (lane 4, 50 μM), proteolytic cleavage of the MBP moiety with TEV protease results in active Igy (lane 5) at concentrations of 12.5 μM and upward (lanes 6 through 8).

(B) *In vitro* cleavage assay. Under cleavage assay conditions, reaction products are treated with SDS/protease K mixture to free DNA ends and visualize DNA cleaved by gyrase. The bottom table shows the compounds present in each lane. PAO1 GyrB (100 nM) was pre-incubated for 15 min on ice with CFX, and then MBP-Igy or Igy were added and reactions were further incubated for 1 h at 30°C. Cleavage complex stabilization by CFX (30 μM) results in the formation of linear DNA (lane 2), resulting in an additional band, whereas the intensity of the relaxed circular DNA band decreases, compared to the control (lane 1). When CFX is incubated together with purified Igy, supercoiled (Sc.) DNA and the gyrase, less linear DNA is produced, leaving more DNA in the relaxed, circular state (lane 4). This finding is compatible with Igy preventing DNA binding and thus cleavage by CFX. The MBP-Igy fusion remains inactive and serves as a negative control (lane 3). Notation for different plasmid topologies is added to the gel, as follows: RC, relaxed circular; Lin, linear; CC, closed circular.

independent clones, and a change from threonine in position 32 to proline was found in two isolates (Figure S4). The mutations affect the charge or the structure of the predicted Igy alpha helix, which mimics DNA.

Most DNA mimics that interfere with gyrase function are pentapeptide repeat (PR) proteins (reviewed by Shah and Heddle, 2014). Unlike other DNA mimics such as P56 that mainly mimic a small part of the negative charge from the phosphate backbone, the PR proteins mimic a larger part of the DNA structure. Igy does not have predicted pentapeptide repeats and could thus be another type of small DNA mimic to inhibit the DNA gyrase.

GyrB is not essential for LUZ24 infection of *P. aeruginosa*

Our results imply that host gyrase is inactivated by LUZ24 during the infection. To establish if this inhibition is necessary for phage development, we performed phage infection in the presence of CFX. As a control, infection with the unrelated *Phikmvvirus* LUZ19 was carried out (Ceyssens et al., 2011). In the case of LUZ19, the production of progeny phage was severely (~1,000-fold) suppressed by the treatment with CFX, whereas LUZ24 progeny production was affected only by 10-fold (Figure 7). However, because we cannot exclude that CFX treatment adversely affects cell growth generally suppressing phage production, we consider the result presented in Figure 7 as an indication that unlike LUZ19, LUZ24 is able to complete its infection cycle without the host gyrase. In the past, other phages have already been found to also function in the presence of nalidixic acid, a quinolone antibiotic that shuts down gyrase activity (Baird et al., 1972). At the same time, other examples exist of early phage proteins interfering with topoisomerases in their host to alter DNA topology, like the T4 ORF 55.2 protein that interacts with topoisomerase I or the recently identified Gip peptide of *Corynebacterium glutamicum* (Kever et al., 2021; Mattenberger et al., 2015). So far, the exact biological role of these inhibitors during phage replication remains elusive, although Mattenberger et al., 2015 propose that T4 gp*55.2* acts as a subtle modulator of topoisomerase activity, and thus DNA topology, when expressed from the phage genome to ensure optimal phage yield. Given the current focus on the functional characterization of Igy as a standalone peptide, future research will have to explore the role Igy would play during phage infection.

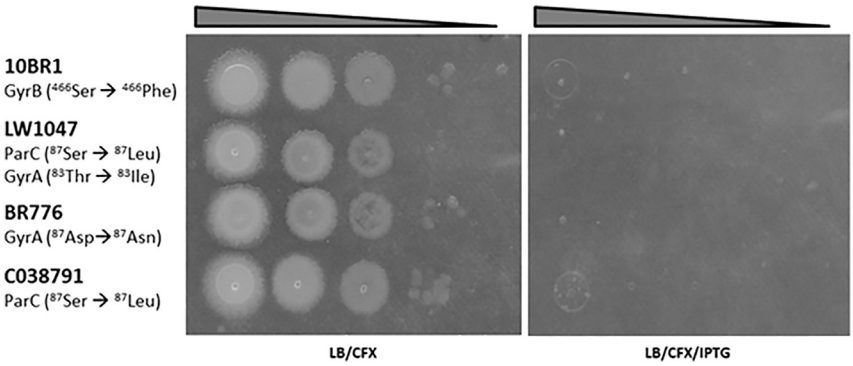

Figure 5. *P. aeruginosa* exhibits no cross-resistance between Igy and CFX in CFX-resistant mutants

On the left, the tested strains are listed together with their specific point mutations, conferring CFX resistance. In each of these strains, an isopropyl-β-D-thiogalactoside (IPTG)-inducible Igy expression cassette was cloned. A dilution series spot test of these strains on LB/ciprofloxacin medium in the presence (right) or absence (left) of IPTG, leading to Igy expression, was performed two times and shows Igy toxicity is independent of the indicated point mutations, proving there is no cross-resistance between both gyrase inhibitors.

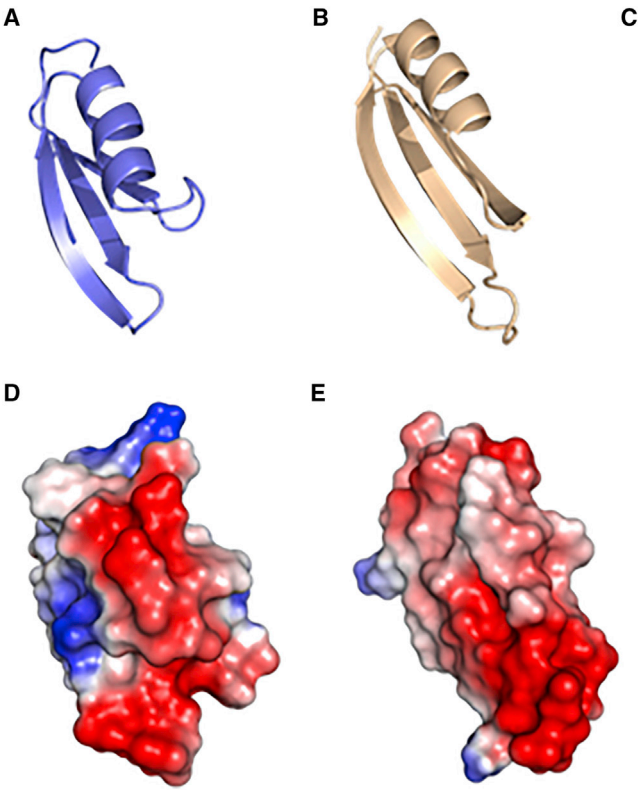

Figure 6. Model of Igy and comparison to P56 of phi29

(A) *De novo* model of Igy as generated by QUARK.
(B) Structure model of a P56 monomer from phi29 (PDB: 3ZOQ).
(C) Overlay of Igy and P56.
(D and E) Electrostatic surface potential of Igy and P56, respectively (generated by PyMOL vacuum electrostatics) with negative charges in red and positive in blue.

Conclusions and perspectives

In silico, the previously described toxic 5.6-kDa peptide Igy of LUZ24 was found to be conserved among the *Bruynoghevirus*. *In vitro* pull-down of Igy with *P. aeruginosa* lysate lead to the co-purification of GyrB. Furthermore, overexpression of the proteases TldDE was shown to alleviate Igy toxicity.

A B2H screen confirmed the interaction of Igy with a GyrB fragment. Moreover, an *in vitro* gyrase activity assay showed that Igy inhibits gyrase supercoiling activity. The *in vitro* gyrase activity assays also suggested a distinct mode of gyrase activity inhibition compared to the well-known class of fluoroquinolone antibiotics, which was further supported by the ability of Igy to prevent the effect of fluoroquinolones on the gyrase complex in a cleavage assay. Finally, four fluoroquinolone-resistant mutants remained sensitive to Igy. When combining these observations with the *de novo* Igy model, we conclude that Igy most likely inhibits gyrase activity by interfering with its ability to bind DNA by DNA mimicry.

A question remains regarding what the biological function of a peptide like Igy during phage infection could be. It was revealed that LUZ24 is able to replicate, albeit less efficiently, in the presence of fluoroquinolones, i.e., in the absence of active host gyrase. More research is needed to explore to what extent Igy is expressed during phage infection and how stable it is in the bacterial cell to assess its exact biological role during phage infection. Be that as it may, our findings do add another example to the growing list of phage-encoded peptides that can affect enzymes regulating DNA topology in their host, illustrating the importance of this host function for optimal phage infection. It is also intriguing to see different examples of peptides encoded by *Enterobacteriaceae* phages affecting either the enzyme responsible for removing or introducing negative supercoils in the DNA, which suggests a complex interaction at this level that warrants further exploration.

We submit that Igy holds potential for the development of novel antibiotics. It targets the DNA gyrase, a known and proven antibacterial target for which a lot of research data are available, which may significantly shorten its potential road to market. Developing small molecules that mimic the action of this inhibitory peptide could prove relevant because the interaction with the DNA gyrase complex has emerged by a long-term co-evolution between phage and bacterial host. One may also envision biotechnological purposes of the peptide itself, as a direct regulator of DNA replication in SynBio applications.

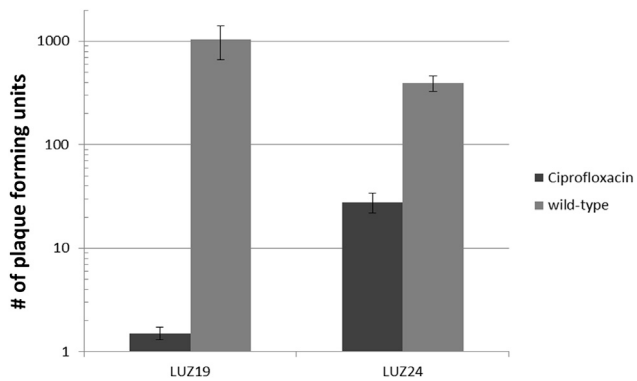

Figure 7. Number of phage particles formed for LUZ19 and LUZ24 in the presence of CFX

On the y axis, the number of formed phage particles is shown. This test was performed in triplicate (n = 3), with the error bars indicating the standard deviation.

STAR★METHODS

Detailed methods are provided in the online version of this paper and include the following:

- KEY RESOURCES TABLE
- RESOURCE AVAILABILITY

SUPPLEMENTAL INFORMATION

Supplemental information can be found online at https://doi.org/10.1016/j.celrep.2021.109567.

ACKNOWLEDGMENTS

The authors would like to thank Prof. Daniel De Vos (Queen Astrid Military Hospital, Brussels, Belgium) for providing the used ciprofloxacin-resistant *P. aeruginosa* strains. The MALDI measurements were carried out by Dr. Marina Serebryakova (A.N. Belozersky Institute of Physico-Chemical Biology, Moscow State University, Russia). J.D.S. held a predoctoral fellowship of the "Agentschap voor Innovatie door Wetenschap en Technologie in Vlaanderen" (IWT, Belgium) and now holds a junior postdoctoral fellowship from the "Fonds Wetenschappelijk Onderzoek" (FWO). This research was also supported by grant G.0323.09 from the FWO and the KU Leuven project GOA "Phage Biosystems."

AUTHOR CONTRIBUTIONS

Conceptualization, J.D.S., P.-J.C., and R.L.; methodology, J.W., D.G., P.-J.C., and R.L.; investigation, J.D.S., M.B., J.W., P.-J.C., M.V., J.A., and D.G.; writing – original draft, J.D.S. and M.B.; writing – review & editing, J.D.S., M.B., J.W., R.L., K.S., and D.G.; funding acquisition, R.L. and K.S.; resources, J.-P.N. and M.V.; supervision, R.L. and K.S.

DECLARATION OF INTERESTS

The authors declare no conflict of interest.

Received: October 30, 2020
Revised: May 20, 2021
Accepted: July 29, 2021
Published: August 24, 2021

REFERENCES

Allali, N., Afif, H., Couturier, M., and Van Melderen, L. (2002). The highly conserved TldD and TldE proteins of *Escherichia coli* are involved in microcin B17 processing and in CcdA degradation. J. Bacteriol. *184*, 3224–3231.

Bae, B., Davis, E., Brown, D., Campbell, E.A., Wigneshweraraj, S., and Darst, S.A. (2013). Phage T7 Gp2 inhibition of *Escherichia coli* RNA polymerase involves misappropriation of σ70 domain 1.1. Proc. Natl. Acad. Sci. USA *110*, 19772–19777.

Baird, J.P., Bourguignon, G.J., and Sternglanz, R. (1972). Effect of nalidixic acid on the growth of deoxyribonucleic acid bacteriophages. J. Virol. *9*, 17–21.

Baños-Sanz, J.I., Mojardín, L., Sanz-Aparicio, J., Lázaro, J.M., Villar, L., Serrano-Heras, G., González, B., and Salas, M. (2013). Crystal structure and functional insights into uracil-DNA glycosylase inhibition by phage Φ29 DNA mimic protein p56. Nucleic Acids Res. *41*, 6761–6773.

Ceyssens, P.-J., Hertveldt, K., Ackermann, H.W., Noben, J.P., Demeke, M., Volckaert, G., and Lavigne, R. (2008). The intron-containing genome of the lytic *Pseudomonas* phage LUZ24 resembles the temperate phage PaP3. Virology *377*, 233–238.

Bruchmann, S., Dötsch, A., Nouri, B., Chaberny, I.F., and Häussler, S. (2013). Quantitative contributions of target alteration and decreased drug accumulation to *Pseudomonas aeruginosa* fluoroquinolone resistance. Antimicrob. Agents Chemother. *57*, 1361–1368.

Ceyssens, P.-J., Glonti, T., Kropinski, N.M., Lavigne, R., Chanishvili, N., Kulakov, L., Lashkhi, N., Tediashvili, M., and Merabishvili, M. (2011). Phenotypic and genotypic variations within a single bacteriophage species. Virol. J. *8*, 134.

Chatterji, M., and Nagaraja, V. (2002). GyrI: a counter-defensive strategy against proteinaceous inhibitors of DNA gyrase. EMBO Rep. *3*, 261–267.

Choi, K.-H., Gaynor, J.B., White, K.G., Lopez, C., Bosio, C.M., Karkhoff-Schweizer, R.R., and Schweizer, H.P. (2005). A Tn7-based broad-range bacterial cloning and expression system. Nat. Methods *2*, 443–448.

Collin, F., and Maxwell, A. (2019). The Microbial Toxin Microcin B17: Prospects for the Development of New Antibacterial Agents. J. Mol. Biol. *431*, 3400–3426.

Claessen, D., Emmins, R., Hamoen, L.W., Daniel, R.A., Errington, J., and Edwards, D.H. (2008). Control of the cell elongation-division cycle by shuttling of PBP1 protein in *Bacillus subtilis*. Mol. Microbiol. *68*, 1029–1046.

Collin, F., Karkare, S., and Maxwell, A. (2011). Exploiting bacterial DNA gyrase as a drug target: current state and perspectives. Appl. Microbiol. Biotechnol. *92*, 479–497.

De Smet, J., Hendrix, H., Blasdel, B.G., Danis-Wlodarczyk, K., and Lavigne, R. (2017). *Pseudomonas* predators: understanding and exploiting phage-host interactions. Nat. Rev. Microbiol. *15*, 517–530.

Fàbrega, A., Madurga, S., Giralt, E., and Vila, J. (2009). Mechanism of action of and resistance to quinolones. Microb. Biotechnol. *2*, 40–61.

Feng, L., Mundy, J.E.A., Stevenson, C.E.M., Mitchenall, L.A., Lawson, D.M., Mi, K., and Maxwell, A. (2021). The pentapeptide-repeat protein, MfpA, interacts with mycobacterial DNA gyrase as a DNA T-segment mimic. Proc. Natl. Acad. Sci. USA *118*, e2016705118.

Flatman, R.H., Howells, A.J., Heide, L., Fiedler, H.P., and Maxwell, A. (2005a). Simocyclinone D8, an inhibitor of DNA gyrase with a novel mode of action. Antimicrob. Agents Chemother. *49*, 1093–1100.

Ghilarov, D., Serebryakova, M., Stevenson, C.E.M., Hearnshaw, S.J., Volkov, D.S., Maxwell, A., Lawson, D.M., and Severinov, K. (2017). The Origins of Specificity in the Microcin-Processing Protease TldD/E. Structure *25*, 1549–1561.e5.

Hartmann, S., Gubaev, A., and Klostermeier, D. (2017). Binding and Hydrolysis of a Single ATP Is Sufficient for N-Gate Closure and DNA Supercoiling by Gyrase. J. Mol. Biol. *429*, 3717–3729.

Hegde, S.S., Vetting, M.W., Mitchenall, L.A., Maxwell, A., and Blanchard, J.S. (2011). Structural and biochemical analysis of the pentapeptide repeat protein EfsQnr, a potent DNA gyrase inhibitor. Antimicrob. Agents Chemother. *55*, 110–117.

Higgins, N.P., Peebles, C.L., Sugino, A., and Cozzarelli, N.R. (1978). Purification of subunits of *Escherichia coli* DNA gyrase and reconstitution of enzymatic activity. Proc. Natl. Acad. Sci. USA *75*, 1773–1777.

Jacobs, M.A., Alwood, A., Thaipisuttikul, I., Spencer, D., Haugen, E., Ernst, S., Will, O., Kaul, R., Raymond, C., Levy, R., et al. (2003). Comprehensive transposon mutant library of *Pseudomonas aeruginosa*. Proc. Natl. Acad. Sci. USA *100*, 14339–14344.

Karimova, G., Pidoux, J., Ullmann, A., and Ladant, D. (1998). A bacterial two-hybrid system based on a reconstituted signal transduction pathway. Proc. Natl. Acad. Sci. USA *95*, 5752–5756.

Keller, A.N., Yang, X., Wiedermannová, J., Delumeau, O., Krásný, L., and Lewis, P.J. (2014). ε, a new subunit of RNA polymerase found in gram-positive bacteria. J. Bacteriol. *196*, 3622–3632.

Kever, L., Hünnefeld, M., Brehm, J., Heermann, R., and Frunzke, J. (2021). Identification of Gip as a novel phage-encoded gyrase inhibitor protein featuring a broad activity profile. bioRxiv. https://doi.org/10.1101/2021.01.28.428610.

Khan, T., Sankhe, K., Suvarna, V., Sherje, A., Patel, K., and Dravyakar, B. (2018). DNA gyrase inhibitors: Progress and synthesis of potent compounds as antibacterial agents. Biomed. Pharmacother. *103*, 923–938.

Krissinel, E., and Henrick, K. (2004). Secondary-structure matching (SSM), a new tool for fast protein structure alignment in three dimensions. Acta Crystallogr. D Biol. Crystallogr. *60*, 2256–2268.

Lammens, E., Ceyssens, P.J., Voet, M., Hertveldt, K., Lavigne, R., and Volckaert, G. (2009). Representational Difference Analysis (RDA) of bacteriophage genomes. J. Microbiol. Methods *77*, 207–213.

Lee, S.W., Mitchell, D.A., Markley, A.L., Hensler, M.E., Gonzalez, D., Wohlrab, A., Dorrestein, P.C., Nizet, V., and Dixon, J.E. (2008). Discovery of a widely distributed toxin biosynthetic gene cluster. Proc. Natl. Acad. Sci. USA *105*, 5879–5884.

Liu, J., Dehbi, M., Moeck, G., Arhin, F., Bauda, P., Bergeron, D., Callejo, M., Ferretti, V., Ha, N., Kwan, T., et al. (2004). Antimicrobial drug discovery through bacteriophage genomics. Nat. Biotechnol. *22*, 185–191.

Mattenberger, Y., Silva, F., and Belin, D. (2015). 55.2, a phage T4 ORFan gene, encodes an inhibitor of *Escherichia coli* topoisomerase I and increases phage fitness. PLoS One *10*, e0124309.

Mazurek, Ł., Ghilarov, D., Michalczyk, E., Pakosz, Z., Metelev, M., Czyszczoń, W., Wawro, K., Behroz, I., Dubiley, S., Süssmuth, R.D., and Heddle, J.G. (2021). Pentapeptide repeat protein QnrB1 requires ATP hydrolysis to rejuvenate poisoned gyrase complexes. Nucleic Acids Res. *49*, 1581–1596.

Metelev, M., Serebryakova, M., Ghilarov, D., Zhao, Y., and Severinov, K. (2013). Structure of microcin B-like compounds produced by *Pseudomonas syringae* and species specificity of their antibacterial action. J. Bacteriol. *195*, 4129–4137.

Morais Cabral, J.H., Jackson, A.P., Smith, C.V., Shikotra, N., Maxwell, A., and Liddington, R.C. (1997). Crystal structure of the breakage-reunion domain of DNA gyrase. Nature *388*, 903–906.

Nakanishi, A., Oshida, T., Matsushita, T., Imajoh-Ohmi, S., and Ohnuki, T. (1998). Identification of DNA gyrase inhibitor (GyrI) in *Escherichia coli*. J. Biol. Chem. *273*, 1933–1938.

Pirnay, J.-P., Bilocq, F., Pot, B., Cornelis, P., Zizi, M., Van Eldere, J., Deschaght, P., Vaneechoutte, M., Jennes, S., Pitt, T., and De Vos, D. (2009). *Pseudomonas aeruginosa* population structure revisited. PLoS One *4*, e7740.

Pirnay, Jean-Paul, De Vos, Daniel, Cochez, Christel, Bilocq, Florence, Vanderkelen, Alain, Zizi, Martin, Ghysels, Bart, and Cornelis, Pierre (2002). *Pseudomonas aeruginosa* displays an epidemic population structure. environmental microbiology *4*, 898–911. https://doi.org/10.1046/j.1462-2920.2002.00321.x.

Projan, S. (2004). Phage-inspired antibiotics? Nat. Biotechnol. *22*, 167–168.

Qiu, D., Damron, F.H., Mima, T., Schweizer, H.P., and Yu, H.D. (2008). P_{BAD}-based shuttle vectors for functional analysis of toxic and highly regulated genes in *Pseudomonas* and *Burkholderia* spp. and other bacteria. Appl. Environ. Microbiol. *74*, 7422–7426.

Ruiz, J. (2019). Transferable mechanisms of quinolone resistance from 1998 onward, e00007-19. Clin. Microbiol. Rev. *32*.

Schoeffler, A.J., May, A.P., and Berger, J.M. (2010). A domain insertion in *Escherichia coli* GyrB adopts a novel fold that plays a critical role in gyrase function. Nucleic Acids Res. *38*, 7830–7844.

Shah, S., and Heddle, J.G. (2014). Squaring up to DNA: pentapeptide repeat proteins and DNA mimicry. Appl. Microbiol. Biotechnol. *98*, 9545–9560.

Shevchenko, A., Wilm, M., Vorm, O., and Mann, M. (1996). Mass spectrometric sequencing of proteins silver-stained polyacrylamide gels. Anal. Chem. *68*, 850–858.

Stover, C.K., Pham, X.Q., Erwin, A.L., Mizoguchi, S.D., Warrener, P., Hickey, M.J., Brinkman, F.S., Hufnagle, W.O., Kowalik, D.J., Lagrou, M., et al. (2000). Complete genome sequence of *Pseudomonas aeruginosa* PAO1, an opportunistic pathogen. Nature *406*, 959–964.

Tomašić, T., and Mašič, L.P. (2014). Prospects for developing new antibacterials targeting bacterial type IIA topoisomerases. Curr. Top. Med. Chem. *14*, 130–151.

Van den Bossche, A., Ceyssens, P.-J., De Smet, J., Hendrix, H., Bellon, H., Leimer, N., Wagemans, J., Delattre, A.-S., Cenens, W., Aertsen, A., et al. (2014). Systematic identification of hypothetical bacteriophage proteins targeting key protein complexes of *Pseudomonas aeruginosa*. J. Proteome Res. *13*, 4446–4456.

Van Melderen, L., Bernard, P., and Couturier, M. (1994). Lon-dependent proteolysis of CcdA is the key control for activation of CcdB in plasmid-free segregant bacteria. Mol. Microbiol. *11*, 1151–1157.

Vos, S.M., Lyubimov, A.Y., Hershey, D.M., Schoeffler, A.J., Sengupta, S., Nagaraja, V., and Berger, J.M. (2014). Direct control of type IIA topoisomerase activity by a chromosomally encoded regulatory protein. Genes Dev. *28*, 1485–1497.

Wagemans, J., Blasdel, B.G., Van den Bossche, A., Uytterhoeven, B., De Smet, J., Paeshuyse, J., Cenens, W., Aertsen, A., Uetz, P., Delattre, A.-S., et al. (2014). Functional elucidation of antibacterial phage ORFans targeting *Pseudomonas aeruginosa*. Cell. Microbiol. *16*, 1822–1835.

Wagemans, J., Delattre, A.-S., Uytterhoeven, B., De Smet, J., Cenens, W., Aertsen, A., Ceyssens, P.-J., and Lavigne, R. (2015). Antibacterial phage ORFans of *Pseudomonas aeruginosa* phage LUZ24 reveal a novel MvaT inhibiting protein. Front. Microbiol. *6*, 1242.

Weidlich, D., and Klostermeier, D. (2020). Functional interactions between gyrase subunits are optimized in a species-specific manner. J. Biol. Chem. *295*, 2299–2312.

Wigley, D.B., Davies, G.J., Dodson, E.J., Maxwell, A., and Dodson, G. (1991). Crystal structure of an N-terminal fragment of the DNA gyrase B protein. Nature *351*, 624–629.

Xu, D., and Zhang, Y. (2012). Ab initio protein structure assembly using continuous structure fragments and optimized knowledge-based force field. Proteins *80*, 1715–1735.

Xu, D., and Zhang, Y. (2013). Toward optimal fragment generations for ab initio protein structure assembly. Proteins *81*, 229–239.

Yin, Y., and Fischer, D. (2008). Identification and investigation of ORFans in the viral world. BMC Genomics *9*, 24.

Zhang, X., and Bremer, H. (1995). Control of the *Escherichia coli* rrnB P1 promoter strength by ppGpp. J. Biol. Chem. *270*, 11181–11189.

Zhao, X., Li, G., and Liang, S. (2013). Several affinity tags commonly used in chromatographic purification. J. Anal. Methods Chem. *2013*, 581093.

STAR★METHODS

KEY RESOURCES TABLE

REAGENT or RESOURCE	SOURCE	IDENTIFIER
Bacterial and virus strains		
E. coli TOP10	ThermoFisher Scientific	C404010
E. coli BL21 (DE3) pLysS	ThermoFisher Scientific	C606003
E. coli BTH101	Euromedex	EUK001
P. aeruginosa PAO1	Stover et al., 2000	N/A
P. aeruginosa PAO1 Δlon	Seattle transposon library	29158
P. aeruginosa Li010	(Pirnay et al., 2002)	N/A
P. aeruginosa BR776	Queen Astrid Military Hospital, Belgium	N/A
P. aeruginosa 10BR1	Queen Astrid Military Hospital, Belgium	N/A
P. aeruginosa Co380791	Queen Astrid Military Hospital, Belgium	N/A
P. aeruginosa Lw1047	Queen Astrid Military Hospital, Belgium	N/A
LUZ24 (GenBank: NC_010325)	Ceyssens et al., 2008	NC_010325
LUZ19 (GenBank: NC_010326)	Lammens et al., 2009	NC_010326
Chemicals, peptides, and recombinant proteins		
Human rhinovirus 3C Protease	Novagen	Cat#71493-3
AcTEV	Invitrogen	Cat#10216572
TldD/E	Lee et al., 2008	N/A
LUZ24 gp9	This paper	N/A
LUZ24 gp9-GST	This paper	N/A
LUZ24 gp9-MBP	This paper	N/A
PAO1 GyrA/B	This paper	N/A
Critical commercial assays		
TA cloning kit	Thermofisher Scientific	Cat#K456001
BACTH System kit	Euromedex	EUK001
Deposited data		
Model PDB ID 3ZOQ	Baños-Sanz et al., 2013	PDB ID: 3ZOQ
Model PDB ID 4NJC	Keller et al., 2014	PDB ID: 4NJC
Model PDB ID 4LK0	Bae et al., 2013	PDB ID: 4LK0
Oligonucleotides		
See Table S3		N/A
Recombinant DNA		
pColA	Merck	N/A
pUC18-mini-Tn7T-Lac	Choi et al., 2005	N/A
pGEX-6P-1-LUZ24 gp9	This paper	N/A
pHERD20T -*P. aeruginosa* genome library	This paper	N/A
pET28-MBP-LUZ24 gp9	This paper	N/A
pTNS2	Choi et al., 2005	N/A
pUT18	Euromedex	EUK001
pUT18C	Euromedex	EUK001
pN-25	Euromedex	EUK001
pKT25	Euromedex	EUK001
pCR8/GW/TOPO	ThermoFisher	Cat#K250020
pET-19b	Novagen	Cat#69677-3

(*Continued on next page*)

Continued

REAGENT or RESOURCE	SOURCE	IDENTIFIER
Software and algorithms		
Scaffold	Proteome Software	http://www.proteomesoftware.com/products/scaffold-5
Sequencher	Gene Codes	https://www.genecodes.com/free-download
FlexAnalysis 3.2 software	Bruker Daltonik	https://bruker-daltonics-flexanalysis.software.informer.com/3.4/
QUARK	Xu and Zhang, 2012, 2013	https://zhanglab.ccmb.med.umich.edu/QUARK/
PDBeFold	Krissinel and Henrick, 2004	https://www.ebi.ac.uk/msd-srv/ssm/
PyMOL	Schrödinger	https://sourceforge.net/projects/pymol/

RESOURCE AVAILABILITY

Lead contact

Further information and requests for resources and reagents should be directed to and will be fulfilled by the lead contact, Prof. Rob Lavigne (rob.lavigne@kuleuven.be)

Materials availability

Generated plasmids and strains are available at the Laboratory of Gene Technology, KU Leuven upon request after completion of an MTA. Contact Prof. Rob Lavigne (rob.lavigne@kuleuven.be) for any further information.

Data and code availability

- All data reported in this paper will be shared by the lead contact upon request.
- This paper does not report original code.
- Any additional information required to reanalyze the data reported in this paper is available from the lead contact upon request

EXPERIMENTAL MODEL AND SUBJECT DETAILS

Bacterial strains

E. coli TOP10 (ThermoFisher Scientific) was used for cloning, *E. coli* BL21 (DE3) pLysS (ThermoFisher Scientific) for recombinant protein expression and *E. coli* BTH101 (Euromedex, Souffelweyersheim, FR) for the bacterial two-hybrid assays. *P. aeruginosa* PAO1 (Stover et al., 2000) was routinely used. To analyze cross-resistance of gp9, four fluoroquinolone resistant strains were used: BR776 (^{87}Asp → ^{87}Asn in GyrA), 10BR1 (^{466}Ser → ^{466}Phe in GyrB), Co380791 (^{87}Ser → ^{87}Leu in ParC) and Lw1047 (^{83}Thr → ^{83}Ile in GyrA & ^{87}Ser → ^{87}Leu in ParC) (Pirnay et al., 2009). The Lon knock-out strain was ordered from the Seattle *P. aeruginosa* PAO1 transposon mutant library (Jacobs et al., 2003). All these microbes can be cultivated in LB broth at a temperature of 37°C.

All *P. aeruginosa* mutants containing an isopropyl-β-D-thiogalactoside (IPTG) inducible chromosomal copy of a phage ORF were constructed and grown according to Wagemans et al., 2014, (Wagemans et al., 2015), using the pUC18-mini-Tn7T-Lac vector (Choi et al., 2005).

Phages

LUZ24 was amplified on *P. aeruginosa* Li010 using the soft agar overlay method, followed by PEG8000 precipitation (Ceyssens et al., 2008). While LUZ19 was amplified on *P. aeruginosa* PAO1 following the same protocol. Produced phages were stored in phage buffer (10 mM Tris pH 7.5, 10 mM $MgSO_4$, 150 mM NaCl) at 4°C. The number of phages was estimated by plating a dilution series of the phage with the soft agar overlay method and counting of the number of plaque forming units (pfu).

METHOD DETAILS

In vivo toxicity analysis

To determine *in vivo* toxicity of LUZ24 gp9 in the presence of *E. coli* or *P. aeruginosa* gyrase (subunits), the gp9 gene was amplified from LUZ24 genomic DNA and cloned into *Pseudomonas* shuttle vector pHERD20T between the NcoI and XbaI restriction sites. To produce plasmid pColA-PAO1/*E. coli*-gyrAB, the GyrA and GyrB subunits were PCR amplified and cloned into multiple cloning sites I

and II, respectively, of the pColA vector (Merck). To calculate colony forming units (CFU) upon gp9 induction in *E. coli*, cultures supplemented by kanamycin and tetracycline were grown to an OD_{600} of 0.4 and protein expression was induced by 1 mM IPTG and 1 mM arabinose. Cells were plated to count CFUs immediately before induction, and 3, 9 and 24 hours later.

In vitro pull-down analysis

For recombinant expression of gp9 using a GST-tag, the corresponding gene was cloned in expression vector pGEX-6P-1 (Cytiva). After transformation to *E. coli* BL21, a 1 L culture was grown to exponential phase (OD_{600} 0.6) before it was induced with 1 mM IPTG for 4 h at 37°C. Cells were pelleted (4,000 g, 45 min, 4°C) and lysed in lysis buffer (20 mM NaH_2PO_4, 0,5 M NaCl, 0.5 mg/ml Henn Egg White Lysozyme, at pH = 7.4) and by sonication. Purification was done using a 5 mL GSTrap HP column (Cytiva) on an Äkta Fast Protein Liquid Chromatograph (FPLC, Cytiva). After equilibration (5 ml/min) with two column volumes (CV) of PBS (137 mM NaCl, 2.7 mM KCl, 10 mM Na_2HPO_4 and 1.8 mM KH_2PO_4, pH 7.5), the lysate was loaded at 1 ml/min, followed by a washing step with four CV of PBS at 3 ml/min. Next, the protein was eluted using elution buffer (50 mM Tris pH 8.0, 10 mM reduced glutathione) at a flow rate of 2 ml/min in twenty 0.5 mL fractions. To remove the Glutathione-S-transferase (GST)-tag, the 5 mL Pall 'Microsep Advance Centrifugal devices' were used according to the manufacturer's protocol to concentrate and dialyse the purified protein to protease restriction buffer (50 mM Tris, 150 mM NaCl, 1 mM EDTA, 1 mM dithiothreitol). Next, 1 U of the human rhinovirus 3C (HRV3C) Protease (2 U/ μl; Novagen) was added per 400 μg of GST-tagged protein and incubated overnight at 4°C to cleave the protein from the GST-tag. Final purification of pure phage protein was done with size exclusion chromatography using a HiLoad 16/600 Superdex 75 Prep grade gel filtration column (Cytiva). After an equilibration with one CV (124 ml) of PBS at 1 ml/min, the protein sample was loaded at the same speed and 120 1 mL fractions were collected. The samples containing the recombinant protein were finally concentrated as previously described.

Next, to identify the bacterial interaction partners of gp9, an *in vitro* pull-down was performed with this purified GST-tagged phage protein and *P. aeruginosa* PAO1 lysate. For this bacterial lysate, cells were grown in 500 mL LB until an OD_{600} of 0.3, pelleted and resuspended in 10 mL protein A buffer (10 mM Tris pH 8,0, 150 mM NaCl, 0,1% (v/v) NP-40). To this volume, 5 mg lysozyme and 0.46 mg Pefabloc® SC was added. After one freeze-thaw cycle, the mixture was supplemented with 800 μL 10x BugBuster® Protein extraction reagent and 10 μl Benzonase nuclease and incubated at room temperature for 20 min, while being gently agitated. After centrifugation, this lysate was loaded on a 1 mL GSTrap HP column (flowrate of 0.5 ml/min) on an FPLC to remove false-positive binding proteins. The flow-through of the lysate was used for the pull down, while after washing (1 ml/min) the proteins bound to the column were eluted (1 ml/min) and removed. Next, the column was loaded (0.5 ml/min) with *E. coli* BL21 lysate that contains the GST-tagged phage protein and washed (1 ml/min) to remove the non-binding *E. coli* proteins. Next, the *Pseudomonas* lysate was loaded (0.3 ml/min) on this column and washed with PBS in two steps (respectively 0.5 ml/min and 1 ml/min) to remove non-binding *Pseudomonas* proteins. Finally, the phage protein and interacting bacterial proteins were eluted (1 ml/min) with elution buffer in 0.5 mL fractions. Elution fractions were concentrated and analyzed using SDS-PAGE.

Gel slices were excised from the gel at the height of the additional bands and subjected to trypsin digestion (Shevchenko et al., 1996). The protocol for mass spectrometry was performed as described previously (Van den Bossche et al., 2014). An Easy-nLC 1000 liquid chromatograph (Thermo Scientific) that was online-coupled to a mass calibrated LTQ-Orbitrap Velos Pro (Thermo Scientific) was used. MS/MS spectra were searched against a database containing all *P. aeruginosa* PAO1 proteins and all ''stop-to-stop'' protein sequences in all six frames of the LUZ24 genome.

Complementation assay

A random genome fragment library of *P. aeruginosa* PAO1 was constructed to identify bacterial proteins that complement the toxic phage proteins. This library contains genome fragments ranging from 2,000 to 6,000 bp in size, inserted in the pHERD20T vector. Expression of the encoded proteins occurred under control of an arabinose inducible p_{BAD} promoter. To start the assay, 200 ng of the library was transformed to two cultures of the *P. aeruginosa* PAO1 strain containing the pUC18-mini-Tn7T-Lac-LUZ24 gp9 constructs. A dilution series of the transformed cells was plated on LB/Gm^{30}/Cb^{200} agar to determine if the transformation efficiency ensured sufficient coverage of the library. At the same time, 225 μl of the transformation mix was plated on four different plates (2x LB/Gm^{30}/Cb^{200}/ 1 mM IPTG agar and 2x LB/Gm^{30}/Cb^{200}/1 mM IPTG/0.2% L-Ara agar) and incubated overnight at 37°C. Colonies that express complementing bacterial genes should be able to grow in the presence of L-arabinose.

These colonies were inoculated in 150 μl LB/Gm^{30}/Cb^{200} and grown overnight at 37°C. Next, a dilution series (10°, 10^{-2}, 10^{-4}) was spotted on LB/Gm^{30}/Cb^{200} and LB/Gm^{30}/Cb^{200}/1mM IPTG ± 0.2% L-Ara to eliminate false-positive hits. From positive hits, the plasmid was isolated and 50 ng was transformed to the original *P. aeruginosa* PAO1::phage gene strain and a new spot test on LB/Gm^{30}/Cb^{200} and LB/Gm^{30}/Cb^{200}/1mM IPTG ± 0.2% L-Ara to confirm the positive hits. The plasmids of the confirmed positive hits were transformed to *E. coli* TOP10, isolated and sequenced using Sanger sequencing.

In vitro protease test

The gene encoding gp9 was amplified from LUZ24 genomic DNA and cloned to pET28-MBP vector using the BamHI and NotI restriction sites, similarly to Qiu et al., 2008. The actual test was done as previously described (Ghilarov et al., 2017). Briefly, 400 mL of 2xYT medium was grown at 37°C to an OD_{600} of0.5, after which is was induced with 0.5 mM IPTG and grown for three more hours at 37°C to produce the peptide with an N-terminal maltose binding protein (MBP) tag. Afterward, it was purified using

an MBPTrap column (Cytiva). The tag was removed after expression by TEV cleavage (AcTEV, Invitrogen; 1 h at 30°C in 10 mM Tris-Cl pH 7.5, 10 mM DTT, 0.5 mM EDTA) leaving a 3 amino acid linker (SGS). The purified TldDE (0.3 μM) (according to Lee et al., 2008) was added and the mixture was desalted (Zip-Tip, Millipore) and analyzed by mass spectrometry. Therefore, 1 μL aliquots of the desalted *in vitro* reaction mixture were diluted in 10 μL of 0.5% trifluoroacetic acid (TFA). 1 μL of the diluted sample was mixed with 0.5 μL of 2,5-dihydroxybenzoic acid solution (20 mg/ml in 30% acetonitrile, 0.5% TFA) and left to dry on the stainless-steel target plate at room temperature. MALDI-TOF MS analysis was performed on UltrafleXtreme MALDI-TOF-TOF mass spectrometer (Bruker Daltonik, Germany) equipped with Nd laser. The MH+ molecular ions were measured in reflector mode; the accuracy of monoisotopic mass peak measurement was within 30 ppm. Spectra were acquired by averaging of a minimum 1000 laser shots from "sweet spots" of matrix crystals. Spectra of fragmentation were obtained in LIFT mode, the accuracy of daughter ions measurement was within 1 Da range. Mass-spectra were processed with the use of FlexAnalysis 3.2 software (Bruker Daltonik, Germany) and analyzed manually.

Bacterial two-hybrid screen

To confirm and elucidate the interaction between gp9 and the gyrase subunit B, the BACTH System kit was used (Karimova et al., 1998). This system contains four different vectors: two high copy number vectors fused to the N-terminal (pUT18) and C-terminal (pUT18C) end of the T18 domain of adenylate cyclase and two low copy number vectors fused to the N-terminal (pN-25) and C-terminal (pKT25) end of the T25 domain (Claessen et al., 2008).

First, all genes and gene fragments were cloned into the pCR8/GW/TOPO vector as described in the TA Cloning Kit (ThermoFisher Scientific). Next, both phage protein and potential bacterial interaction partners, were subcloned in the four vectors using Gateway cloning (ThermoFisher Scientific). To test potential auto-activation, 10 ng of each construct was co-transformed with 10 ng of its empty counterpart to the adenylate cyclase-deficient *E. coli* reporter strain BTH101. Since these results were negative, all combinations of phage and bacterial genes/fragments were co-transformed. A mixture of three clones of this transformation were grown overnight and a dilution series of this overnight culture was spotted on synthetic minimal M63 medium and incubated for 48h-72h at 30°C. As a positive control for the assay, a combination of pKT25-zip and pUT18C-zip were co-transformed to the reporter cells. This Zip protein is known to form dimers in the leucine zipper of GCN4. Finally, the β-galactosidase activity was determined quantitatively for all positive hits using a Miller assay (Zhang and Bremer, 1995).

In vitro gyrase activity assay

PAO1 GyrA subunit was amplified from chromosomal DNA and cloned into pColA between the BamHI and SacI sites. GyrB, on the other hand, was cloned to pET-19b using the NdeI and XhoI resriction sites. PAO1 gyrase subunits were purified as described elsewhere (Metelev et al., 2013). Briefly, overnight cultures (5 ml) of *E. coli* BL21 (DE3) carrying pColA PAO1-*gyrA* or pET19 PAO1-*gyrB* were grown in LB supplemented with the relevant antibiotics and used to inoculate 0.5 L LB with antibiotic. Cells were grown at 37°C until an OD_{600} of 0.6 was reached and induced by adding IPTG to 0.2 mM. Induced cultures were further grown for 16 h at 22°C. Cells were collected by centrifugation for 10 minutes at 4,000 g and the pellet was resuspended in lysis buffer (20 mM Tris-HCl pH 8, 200 mM $(NH_4)_2SO_4$, 20 mM imidazole, 10% glycerol). Lysozyme was added to the final concentration of 1 mg/ml and the mixture was incubated on ice for 30 min. Cells were lysed by sonication and further centrifuged at 20,000 g for 30 min. The supernatant was applied to a 1 mL HisTrap HP column (Cytiva) equilibrated in lysis buffer. The column was washed extensively with wash buffer (20 mM Tris-HCl pH 8, 200 mM $(NH_4)_2SO_4$, 50 mM imidazole, 10% glycerol), and proteins were eluted with elution buffer (50 mM Tris, pH 8.0, 200 mM $(NH_4)_2SO_4$, 10% glycerol, 300 mM imidazole).

Gp9 was prepared from an affinity purified MBP-tagged fusion by treatment with the TEV protease (Zhao et al., 2013). Without the tag, gp9 was found to be highly unstable. Consequently, after the removal of MBP, the peptide was immediately used for *in vitro* assays.

For the supercoiling assay, which serves to test the impact of compounds on gyrase activity, PAO1 gyrase (10-20 nM) was pre-incubated for at least 15 min on ice with cleaved MBP-Gp9 (at 12.5, 25, 50 μM) in supercoiling assay buffer (35 mM Tris-HCl (pH 7.5), 24 mM KCl, 4 mM $MgCl_2$, 2 mM dithiothreitol (DTT), 1.75 mM ATP, 6.5% glycerol, 1.8 mM spermidine, 0.1 mg/ml albumin). 12.5 nM DNA (pUC19) was added and reactions were incubated for 1 h at 30°C.

For the cleavage assay, which serves to test if a gyrase inhibitor is a "gyrase poison," the amount of gyrase was increased 10-fold. PAO1 GyrB (100 nM) was pre-incubated 15 minutes on ice with ciprofloxacin (CFX) and then the MBP-Igy or Igy were added and reactions were further incubated for 1 hour at 30°C. The reactions were terminated by the addition of SDS (to 0.2%) and proteinase K (to 0.1 mg/ml) to the mixtures, followed by incubation at 37°C for another 30 min to visualize linear DNA fragments.

Gp9 *de novo* modeling and fold comparison

Gp9 structure was modeled by the QUARK *ab initio* protein structure prediction service using the Igy protein sequence as input (Xu and Zhang, 2012, 2013; available at https://zhanglab.ccmb.med.umich.edu/QUARK/). The first model (highest scoring) was selected for further analysis. This model was compared to existing structures across the PDB database with PDBeFold (Krissinel and Henrick, 2004; available at https://www.ebi.ac.uk/msd-srv/ssm). Figures were generated using PyMOL (The PyMOL Molecular Graphics System, Version 2.0 Schrödinger, LLC.).

Spontaneous mutant screening

To identify mutations in the phage gene that abolish toxicity, *P. aeruginosa* PAO1 cells containing the pUC18-mini-Tn7T-Lac-GW cassette with LUZ24 gp9 inserted in their genome were plated overnight on LB agar with 1 mM IPTG. The toxicity of the phage gene prevents bacterial growth, so colonies that did grew are assumed to contain mutations that abolish toxicity. To check this, the pUC18-mini-Tn7T-Lac-GW cassette in these colonies was amplified using PCR and the sequence of both promotor region and the gene was determined using Sanger sequencing.

For the identified mutations, an alternative pUC18-mini-Tn7T-Lac-GW plasmid was constructed by directed mutagenesis, coding the mutated gene, to confirm that this mutation resulted in the loss of toxicity and not from other undetected mutation in the bacterial genome sequence. Briefly, primers were designed that contained the desired mutation and enable amplification of the plasmid. These primers were phosphorylated by adding 4 μl T4 PNK and 1 mM dATP, the mixture was incubated for 1 hour at 37°C, then inactivated for 10 minutes at 70°C and used in a PCR with 9 pg of the original plasmid as template to introduce the mutation. The amplified linear plasmid was extracted from an agarose gel and 25 ng of the purified PCR mix was then incubated with 0.5 μl Quick T4 Ligase in the corresponding buffer. The ligation mix was then transformed to chemically competent *E. coli* TOP10, the encoded plasmid purified and sequenced. If the mutation was correct in the plasmid, it was transformed to *P. aeruginosa* PAO1 for a toxicity spot test.

Construction of expression plasmids and toxicity analysis of truncated peptides

Directed mutagenesis was also used to remove parts of the LUZ24 gp9 coding sequence in the pUC18-mini-Tn7T-Lac-GW plasmid. Once the desired primers were developed, the same protocol as described above was followed.

Phage amplification dependency on functional host gyrase

To test if LUZ24 infection can proceed in the presence of ciprofloxacin (CFX), 60 μl of 1 mM CFX was added to a 3 mL *P. aeruginosa* PAO1 culture at OD_{600} of 0.3, followed by 5 minutes incubation at 37°C. Parallel to a non-spiked culture, the culture was infected with 9.10^7 and 5.10^8 pfu of LUZ19 (Lammens et al., 2009) and LUZ24 (Ceyssens et al., 2008), respectively a multiplicity of infection (MOI) of 0.5-1. After 5 to 10 minutes a 200 μl sample was taken, centrifuged for 30 s and 10 μl of the supernatant was diluted and tittered.

QUANTIFICATION AND STATISTICAL ANALYSIS

All information regarding the statistical testing including number of repeats (n), standard deviations and p values, as well as the types of statistical test used can be found in the figure legends for each data figure, if relevant. More specifically, the Student's t test was used for analyzing significant differences between the Miller Assay results of the Bacterial Two Hybrid analysis (Figure 2). Standard deviations were also calculated for these results, as well as for the *in vivo* toxicity assay represented in Figure 3 and for the analysis of the phage amplification dependency on gyrase in Figure 7. All these calculations were performed in MS Excel.